PHYSICAL REVIEW B, VOLUME 63, 201201(R)

Carbon vacancy-related defect in 4*H* and 6*H* SiC

N. T. Son, P. N. Hai,* and E. Janzén
Department of Physics and Measurement Technology, Linköping University, SE-581 83 Linköping, Sweden
(Received 9 October 2000; revised manuscript received 22 February 2001; published 20 April 2001)

An electron paramagnetic resonance (EPR) spectrum was observed at temperatures above 25 K in *p*-type 4*H* and 6*H* SiC irradiated with electrons. The center has C_{3V} symmetry with an electron spin $S=1/2$. Using high frequency (~95 GHz) EPR it was possible to obtain the detailed hyperfine structure due to the interaction with the four nearest silicon neighbors, and to identify the defect as the carbon vacancy in the positive-charge state (V_{C^+}). The *g* values and hyperfine tensor of the center in both polytypes are almost the same and no dependence on the inequivalent lattice sites has been detected.

DOI: 10.1103/PhysRevB.63.201201 PACS number(s): 61.72.Ji, 61.80.Fe, 61.82.Fk

Vacancies can be introduced during crystal growth or material processing such as electron irradiation for carrier lifetime control or ion implantation for making contact or isolating layers. They often introduce deep levels in the band gap of semiconductors and hence have a strong influence on the electrical and optical properties of the material. In SiC, both the silicon and carbon vacancies are stable at room temperature and are electrically active. The negatively-charged silicon vacancy (V_{Si}^-) has been identified by electron paramagnetic resonance (EPR) in 3C,[1] 4*H* (Ref. 2) and 6*H* SiC.[3] Its high symmetry (T_d) and high spin configuration ($S=3/2$) were also confirmed by theoretical calculations.[4,5] The other charge states of the silicon vacancy appear to be much less known. The photoluminescence centers V_1, V_2 in 4*H* and V_1, V_2, and V_3 in 6*H* SiC (or the P3 and P5 EPR centers in 6*H* SiC, which were previously attributed to long-distance vacancy pairs by Vainer *et al.*[6]) were suggested as to originate from the V_{Si^0} at different inequivalent sites.[7]

The EPR identification of the carbon vacancy (V_C) may be easier compared to the V_{Si} since there is a better chance of detecting the hyperfine structure of ^{29}Si ($I=1/2$, 4.7% natural abundance) than that of ^{13}C ($I=1/2$, 1.16%). In the past, several V_C-related defects have been observed in 3C,[8] 4*H*,[9] and 6*H* SiC,[6,9,10] of which the T5 center in proton-irradiated *p*-type 3C SiC was attributed to the single carbon vacancy in the positive-charge state (V_C^+).[8] The T5 center has D_2 symmetry and is annealed out at around 200 °C. This has led to a general belief that the V_C becomes mobile at this temperature. In contrast to this EPR observation, recent theoretical calculations[5,11] have predicted that the carbon vacancy in SiC is a negative-*U* system and therefore cannot be detected by EPR under equilibrium conditions.

In this work, we used EPR at the *X*-band (~9.5 GHz) and *W*-band (~95 GHz) frequencies to study intrinsic defects in 4*H* and 6*H* SiC. At high frequency, it is possible to separate most of the EPR spectra in 4*H* and 6*H* SiC. An EPR spectrum with a detailed HS due to the interaction with four nearest Si neighbors has been observed. The spectrum is identified as originating from the positively-charged carbon vacancy (V_C^+). The electronic structure and annealing behavior of the center are discussed and compared with that of the T5 center in 3C SiC.

The samples used in this work were mainly commercial *n*- and *p*-type 4*H* and 6*H* SiC substrates and also free-standing *p*-type layers grown high temperature chemical vapor deposition (HTCVD). The *p*-type substrates were Al-doped (2×10^{17}–1×10^{18} cm^{-3}). The *p*-type layers were either Al-doped (in the mid 10^{17} cm^{-3} range) or compensated by residual impurities with a concentration below 10^{16} cm^{-3}. The samples were irradiated with 2.5 MeV electrons at room temperature or at 400 °C with doses in the range of 1×10^{17}–2×10^{18} cm^{-2}. EPR measurements were performed on Bruker *X*-band (~9.5 GHz) EPR spectrometers (ER200D-SRC or ELESYS 580) and also on a homemade *W*-band (~95 GHz) EPR setup. In *W*-band experiments, we used an Oxford, split-coil superconducting magnet (0–5 T) with a liquid He bath cryostat, which allowed temperature regulation in the range from 1.6 K to room temperature. The magnetic field was calibrated using the well-known P_s^0 signal in Si.[12]

In *p*-type 4*H* and 6*H* SiC irradiated with electrons at 400 °C, several EPR spectra were detected. Figures 1(a) and 1(b) show the spectra observed in the 4*H* polytype for the magnetic field **B** parallel to the *c*-axis at *X*-band and *W*-band frequencies, respectively. At *W*-band frequency, two strong lines, labeled EI5 and EI6, are well separated [Fig. 1(b)]. In *p*-type samples irradiated at room temperature, the EI5 and EI6 signals were also detected together with the EI1 and EI2 spectra (the V_C- and V_{Si}-related defects, respectively).[9] To avoid the overlapping between the HF lines of the EI5 and EI6 spectra with the EI1 signal at *W*-band frequency, we used samples irradiated at 400 °C, in which the EI1 center was annealed out. As can be seen in the figures, the distances between the satellites (indicated by arrows) of the EI5 line are the same when measuring at *X*-band and *W*-band frequencies and do not depend on temperature. This confirms that the satellites are the HSs of the EI5 spectrum but not fine structures of a spin $S=1$ center split by the crystal field. The intensity ratio between all four satellites and the main line is about 20%, which is approximately the natural abundance of four ^{29}Si isotopes. The intensity ratio has been checked for spectra measured at different orientations of the magnetic field and the evaluation by comparing either the signal amplitudes or numerical double integration of the peaks gives similar values in the range 18–20.5 %. Therefore, these satellites can be identified as the HSs due to the interaction between the electron spin and the nuclear spin of the ^{29}Si atoms in the NN shell. This structure is typical for the hyperfine interaction with four nearest Si neighbors of an iso-

 ©2001 The American Physical Society

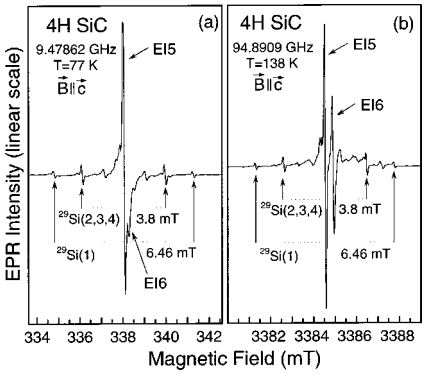

FIG. 1. EPR spectra observed in *p*-type, electron-irradiated 4*H* SiC for the magnetic field **B** parallel to the *c*-axis at (a) *X*-band and (b) *W*-band frequencies.

lated defect at a carbon site. For **B** parallel to the *c*-axis (see Fig. 2), the interaction with the Si(1) atom on the bond along the *c*-axis will be strongest, which gives rise to the two lines with the largest splitting (the two outer hyperfine lines in Fig. 1). The total intensity of these two hyperfine lines is about 4.7% of that of the main line. At this direction of **B**, the three Si atoms on the bonds inclined an angle of 71° [the Si(2,3,4) atoms in Fig. 2] with the *c*-axis are equivalent, and therefore the interactions with these atoms give rise to two hyperfine lines with triple intensity (i.e., about 15%) compared to that of the outer lines.

The spectra in 4*H* and 6*H* SiC measured at *W*-band frequency with **B** in the (1120) plane and perpendicular to the *c*-axis are shown in Figs. 3(a) and 3(b), respectively. The assignment of the hyperfine lines is indicated in the figures. At this direction of **B**, the interaction with the Si(3) and Si(4) atoms (Fig. 2) is equivalent and gives rise to the same lines with double intensity [Fig. 3(b)]. The interaction with the Si(2) atom will be strongest [favored by a larger value of $\cos(\mathbf{B}\cdot\mathbf{c})$] and gives rise to the two lines with the largest splitting (Fig. 3). In the case of 4*H* SiC, due to a small misalignment of the sample, the Si(3) and Si(4) atoms become inequivalent with respect to the magnetic field, and therefore, the corresponding hyperfine lines split off [Fig. 3(a)]. The EI6 and other weak lines in Figs. 1 and 3 belong

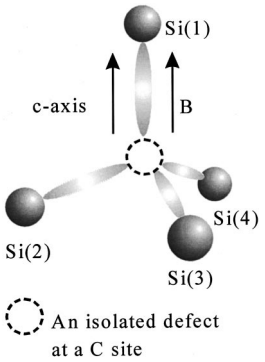

FIG. 2. An isolated defect at a C site with the magnetic field parallel to the *c*-axis. The expected symmetries of the hyperfine tensors representing the interaction with the Si(1) and Si(2,3,4) are C_{3V} and C_{1h}, respectively.

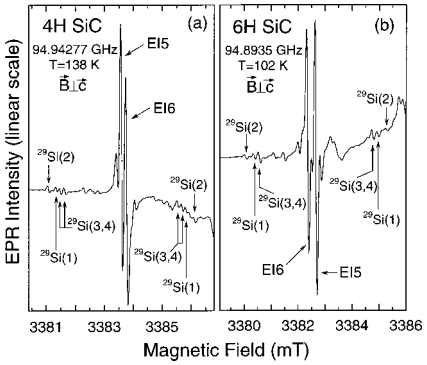

FIG. 3. EPR spectra observed in *p*-type, electron-irradiated (a) 4*H* and (b) 6*H* SiC for the magnetic field **B** perpendicular to the *c*-axis at *W*-band frequencies.

to different defects and will not be discussed in this paper.

In order to determine the symmetry, *g*-values and the hyperfine tensor of the center, the angular dependencies of the spectra were measured by rotating **B** in the (1120) plane. The experimental data in 4*H* and 6*H* SiC are shown as open circles in Figs. 4 and 5, respectively. The angular dependencies of the EI5 center in both polytypes are similar and can be described by the following spin-Hamiltonian

$$H=\mu_B\mathbf{B}\cdot\mathbf{g}\cdot\mathbf{S}+\sum_{j=1-4}\mathbf{S}\cdot\mathbf{A}^{(j)}\cdot\mathbf{I}_{\mathrm{Si}}, \tag{1}$$

with the effective electron spin $S=1/2$. Here μ_B is the Bohr magneton and the *g* tensor is constrained to the trigonal symmetry (C_{3V}) with the principal values $g_\parallel$ and $g_\perp$ corresponding to the values in the [0001] and [1100] directions of the hexagonal lattice. The second term describes the hyperfine interaction with the ^{29}Si nuclei ($I_{\mathrm{Si}}=1/2$) in the NN shell. The hyperfine tensor $A^{(1)}$ represents the hyperfine interaction with the Si(1) atom (see Fig. 2) and has C_{3V} symmetry whereas the hyperfine interaction with other three Si(1,2,3) atoms is described by the same tensor $A^{(2)}$ that has C_{1h} symmetry. The $A^{(2)}$ tensor is described in the principal coordinate system with the principal axes $A_x^{(2)}$ and $A_z^{(2)}$ lying in the $(11\bar{2}0)$ plane and the $A_y^{(2)}$ axis perpendicular to this plane. The angle β between the $A_z^{(2)}$ and the *c*-axis was determined to be 5° for the center in both 4*H* and 6*H* SiC. The parameters deduced from the fit for the EI5 center are given in Table I. The simulated angular dependencies are plotted as solid (for the main line) and dashed curves (for the hyperfine lines) in Figs. 4 and 5, respectively. In the case of 4*H* SiC (Fig. 4), a misorientation angle of 3° in the rotating plane of the magnetic field [**B** was not exactly rotating in the (1120) plane] was included in the fit to account for the splitting induced by sample misalignment.

Following the one-electron linear combination of atomic orbitals approximation, the wave function of the unpaired electron close to a neighboring Si atom can be written as a superposition of the electronic wave function (ψ_s,ψ_p) of the *s* and *p* orbitals of the Si atom

$$\Psi=\eta(\alpha\psi_s+\gamma\psi_p). \tag{2}$$

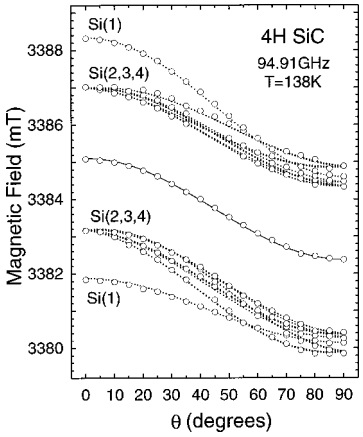

FIG. 4. The angular dependence of the EI5 spectrum in 4*H* SiC measured with **B** rotating in the (1120) plane. θ is the angle between the magnetic field and the *c* axis. (θ=0° and θ=90° correspond to $\mathbf{B}\|\mathbf{c}$ and $\mathbf{B}\perp\mathbf{c}$, respectively).

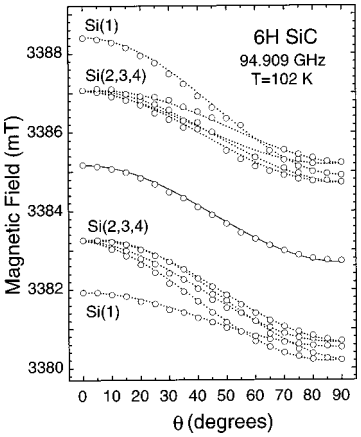

FIG. 5. Angular dependence of the EI5 spectrum in 6*H* SiC.

This wave function gives rise to a hyperfine interaction with isotropic and anisotropic components, which can be related to the unpaired spin in the *s* and *p* orbitals, respectively. The decomposition of the hyperfine tensor into isotropic and anisotropic parts can be written as

$$\mathbf{A}=a\mathbf{1}+\mathbf{b}. \tag{3}$$

The trace *a* of the tensor *A*, the Fermi contact term, is determined by the spin density $\eta^2\alpha^2$ in the *s* orbital by the expression

$$a=(1/3)(A_{\|}+2A_{\perp})=(2/3)\mu_0 g\mu_B g_N\mu_N\eta^2\alpha^2|\psi_s(0)|^2. \tag{4}$$

The traceless anisotropic part **b** is an axial tensor with principal values $(2b,-b,-b)$, where

$$b=(1/3)(A_{\|}-A_{\perp})=(1/4\pi)\mu_0 g\mu_B g_N\mu_N\eta^2\gamma^2(\pm 2/5)\langle r^{-3}\rangle_p. \tag{5}$$

Here μ_N is the nuclear magneton and g_N the nuclear *g*-value of Si. Using atomic constants given by Morton and Preston,[13] g_N value as tabulated by Fuller[14] and hyperfine parameters from Table I, the spin densities $\eta^2\alpha^2$ and $\eta^2\gamma^2$ in the 3*s* and 3*p* orbitals on the Si(1) atom are found to be 0.031 and 0.164, respectively. The $A^{(2)}$ tensor is nearly axial along the *x*-axis and the values $A_{\|}$ and $A_{\perp}$ in Eqs. (4) and (5) are replaced by $A_x^{(2)}$ and $(A_y^{(2)}+A_z^{(2)})/2$, respectively. The corresponding spin densities on each of the three Si atoms (Si atoms 2, 3, and 4 in Fig. 2) are determined as $\eta^2\alpha^2=0.025$ and $\eta^2\gamma^2=0.104$. The localization of the wave function on the Si(1) atom (~19.5%) is larger compared to that on the other nearest Si neighbors (~12.9%).

From the HS due to the interaction with four nearest Si neighbors and the symmetry C_{3V}, it can be concluded that the EI5 center is an isolated defect at a carbon site. The center can only be detected in irradiated materials and the signal intensity increases with the dose of irradiation independently on the concentration of residual impurities (secondary ion mass spectrometry studies of crystals used in this work showed that the concentrations of common impurities such as Al, V, Ti, Cr, B in commercial substrates are one to two orders of magnitude higher than in HTCVD layers). This indicates that the EI5 center is related to intrinsic defects. Therefore, the only model that could explain the observed electronic structure of this isolated intrinsic defect is the carbon vacancy. The V_C can have a spin $S=1/2$ in either the negative or positive charge state. However, since the spectrum only can be detected in *p*-type, irradiated materials, the charge state of the center must be positive. The EI5 center is therefore attributed to the V_C^+.

In all studied samples, the EI5 spectrum was not detectable at temperatures below 25 K. Possibly, when decreasing temperature the Fermi level moves up (away from the valence band) and passes the (+/0) level of the carbon vacancy and therefore the EPR signal of the V_C^+ disappears. No dependence on the inequivalent lattice sites was observed for the EI5 center in both 4*H* and 6*H* SiC. The electronic structure of the EI5 center is very different from that of the T5

TABLE I. Spin-Hamiltonian parameters of the EI5 center in 4*H* and 6*H* SiC. The angle between the principal *z* axis of the $A^{(2)}$ tensor is β=5°. The error in the determination of the *g* values is ±0.000 05.

Polytype	Spin and symmetry	*g*	*A* (MHz)	*a* (MHz)	*b* (MHz)	$\eta^2\alpha^2$	$\eta^2\gamma^2$
4*H*	$S=1/2$	$g_{\|}=2.00322$	$A_{\|}^{(1)}=181.08$, $A_{\perp}^{(1)}=125.01$	143.76	18.69	0.031	0.164
	C_{3V}	$g_{\perp}=2.00484$	$A_x^{(2)}=140.60$, $A_y^{(2)}=103.43$, $A_z^{(2)}=106.73$	116.92	11.84	0.025	0.103
6*H*	$S=1/2$	$g_{\|}=2.00316$	$A_{\|}^{(1)}=181.67$, $A_{\perp}^{(1)}=123.21$	145.70	19.49	0.032	0.171
	C_{3V}	$g_{\perp}=2.00461$	$A_x^{(2)}=140.30$, $A_y^{(2)}=103.43$, $A_z^{(2)}=106.73$	116.82	11.74	0.025	0.103

center in 3C SiC,[8] which has been attributed to the V_C^+. The average *g*-value of the EI5 spectrum (2.0043 and 2.00413 for 4*H* and 6*H* SiC, respectively) is markedly higher than that of the T5 center (~1.99927).[8] The localization of the wave function at the nearest Si neighbors in the case of the EI5 center (~58%) is double compared to that of the T5 center (~29%).[8,15] As the result, the hyperfine constants are also about two times different between the two centers. Detailed annealing behavior was not obtained since at around 450 °C, in both 4*H* and 6*H* SiC, a broad EPR line appears right between the EI5 and EI6 signals making it difficult to know when the EI5 spectra completely vanished. However, at 450 °C the HF lines of the EI5 spectrum are still observable. These HF lines were not detected after annealing at 500 °C (the main line might not be completely disappeared but was significantly decreased so that weak HF lines were not detectable). In recent isochronal annealing studies of 6*H* SiC with positron lifetime, Ling *et al.*[17] also found that the carbon vacancy annealed out in the temperature range 400–650 °C. The annealing behavior of the EI5 center is clearly different from that of the T5 center in 3C SiC, which was annealed out at about 200 °C.[8,15] It should be noticed that the T5 center[8] and EI1 center in 4*H* and 6*H* SiC (Ref. 9) (or the PB center in 6*H* SiC)[10] are very similar in *g*-values, the strength of the hyperfine coupling constants and the annealing behavior. Cha *et al.*[10] attributed the PB center in 6*H* SiC to the V_C^+, in which the unpaired spin locates at one of the two reconstructed Si–Si bonds. At low temperature, the hole (or the unpaired electron) of the V_C^+ may be frozen out in one of the bonds and the defect may have C_{1h} symmetry, but at moderate temperatures the unpaired electron will be shared by four dangling bonds and therefore the defect should have C_{3V} symmetry and a hyperfine interaction with four nearest Si neighbors. The EI1 (or PB) spectrum SiC does not change in symmetry or *g*-values in studied temperature range 4–250 K. Our recent annealing studies of the EI1 spectrum in 4*H* and 6*H* SiC indicate that it starts decreasing at 160–170 °C and seems to transfer to a similar EPR spectrum, which has also C_{1h} symmetry but a slightly different *g*-tensor. After annealing at around 200–220 °C, the spectrum reaches their maximum when the EI1 completely disappears. Both the EI1 and T5 spectra can be detected only in *p*-type, but not even in weakly *n*-type materials under light illumination. Their *g* values and the strength of the HF constants are very similar, but the HF interaction is completely different. The HF interaction is with four nearest Si neighbors in the case of the T5 center in 3C SiC and with only two of the four neighbors in the case of the EI1 center in 4*H* and 6*H* SiC. This clearly indicates that they are not the same defect in different polytypes. Zywietz *et al.*[5] found in their calculations that the V_C^+ in 3C SiC should have D_{2d} but not D_2 symmetry as the T5 center. Calculations of the spin density of the V_C^+ in 3C SiC by Gali *et al.*[16] found a localization of about 16% on each of the Si neighbors compared to 7% deduced from experiments for the T5 center.[8] Unfortunately, there can be an overestimate of the localization due to the restriction of the cluster size on the delocalization of the defect orbitals and therefore a comparison with the calculated value may not be appropriate (the evaluation using different cluster sizes is not available). It is possible that the T5 and EI1 centers may be related to the (V_C+2H) and (V_C+H) complexes, respectively. The low annealing temperature of the T5 and EI1 centers (~200 °C) may be due to mobile hydrogen.

In summary, we have observed in electron-irradiated, *p*-type 4*H* and 6*H* SiC an EPR center, which has C_{3V} symmetry and an electron spin $S=1/2$. Based on the symmetry, the hyperfine structure due to the interaction with four nearest Si neighbors, and the conditions for observation, the defect is identified as the positively-charged carbon vacancy. By changing the charge state (V_C^0 to V_C^+) the carbon vacancy can compensate acceptors in *p*-type material.

Support for this work was provided by the SSF program SiCEP, the Swedish Research Council for Engineering Sciences (TFR), the Swedish Natural Science Research Council (NFR), Okmetic AB, ABB Corporate Research and the National Defense Research Establishment (FOA).

*Present address: Department of Physics, University of Hanoi, 90 Nguyen Trai, Dong da, Hanoi, Vietnam.

[1] H. Itoh, M. Yoshikawa, I. Nashiyama, S. Misawa, H. Okumura, and S. Yoshida, IEEE Trans. Nucl. Sci. **37**, 1732 (1990).

[2] T. Wimbauer, B. K. Meyer, A. Hofstaetter, A. Scharmann, and H. Overhof, Phys. Rev. B **56**, 7384 (1997).

[3] J. Schneider and K. Maier, Physica B **185**, 199 (1993).

[4] L. Torpo, R. M. Nieminen, K. E. Laasonen, and S. Pöykkö, Appl. Phys. Lett. **74**, 221 (1999).

[5] A. Zywietz, J. Furthmüller, and F. Bechstedt, Phys. Rev. B **59**, 15 166 (1999).

[6] V. S. Vainer and A. Il'in, Sov. Phys. Solid State **23**, 2126 (1981).

[7] E. Sörman, N. T. Son, W. M. Chen, O. Kordina, C. Hallin, and E. Janzén, Phys. Rev. B **61**, 2613 (2000).

[8] H. Itoh, M. Yoshikawa, I. Nashiyama, S. Misawa, H. Okumura, and S. Yoshida, J. Electron. Mater. **21**, 707 (1992).

[9] N. T. Son, W. M. Chen, J. L. Lindström, B. Monemar, and E. Janzén, Mater. Sci. Eng., B **61-62**, 202 (1999).

[10] D. Cha, H. Itoh, N. Morishita, A. Kawasuso, T. Oshima, Y. Watanabe, J. Ko, K. Lee, and I. Nashiyama, Mater. Sci. Forum **264-268**, 615 (1998).

[11] F. Bechstedt, A. Zywietz, and J. Furthmüller, Europhys. Lett. **44**, 311 (1998).

[12] G. Feher, Phys. Rev. **114**, 1219 (1959).

[13] J. R. Morton and K. F. Preston, J. Magn. Reson. **30**, 577 (1978).

[14] G. H. Fuller, J. Phys. Chem. Ref. Data **5**, 835 (1976).

[15] H. Itoh, A. Kawasuso, T. Oshima, M. Yoshikawa, I. Nashiyama, S. Tanigawa, S. Misawa, H. Okumura, and S. Yoshida, Phys. Status Solidi A **162**, 173 (1997).

[16] A. Gali, B. Aradi, P. Deák, W. J. Choyke, and N. T. Son, Phys. Rev. Lett. **84**, 4926 (2000).

[17] C. C. Ling, C. D. Beling, and S. Fung, Phys. Rev. B **62**, 8016 (2000).